NASA TECHNICAL MEMORANDUM

NASA TM X-64843

A PROCEDURE FOR CALCULATION OF BOUNDARY LAYER TRIP PROTUBERANCES IN OVEREXPANDED ROCKET NOZZLES

By Robert H. Schmucker

Astronautics Laboratory

April 2, 1973

NASA

George C. Marshall Space Flight Center
Marshall Space Flight Center, Alabama

MSFC - Form 3190 (Rev June 1971)

TECHNICAL REPORT STANDARD TITLE PAGE

1. REPORT NO.	2. GOVERNMENT ACCESSION NO.	3. RECIPIENT'S CATALOG NO.
TM X-64843		

4. TITLE AND SUBTITLE	5. REPORT DATE
A Procedure for Calculation of Boundary Layer Trip Protuberances in Overexpanded Rocket Nozzles	April 2, 1973
	6. PERFORMING ORGANIZATION CODE
7. AUTHOR(S)	8. PERFORMING ORGANIZATION REPORT #
Robert H. Schmucker*	
9. PERFORMING ORGANIZATION NAME AND ADDRESS	10. WORK UNIT NO.
George C. Marshall Flight Center Marshall Space Flight Center, Alabama 35812	11. CONTRACT OR GRANT NO.
	13. TYPE OF REPORT & PERIOD COVERED
12. SPONSORING AGENCY NAME AND ADDRESS	Technical Memorandum
National Aeronautics and Space Administration Washington, D.C. 20546	14. SPONSORING AGENCY CODE

15. SUPPLEMENTARY NOTES

Prepared by Astronautics Laboratory, Science and Engineering

*National Research Council, National Academy of Sciences, Washington, D.C. 20546

16. ABSTRACT

A procedure is described for sizing, scaling, positioning and performance loss calculation of a boundary layer trip protuberance. The theoretical results are compared with some experimental data.

17. KEY WORDS	18. DISTRIBUTION STATEMENT
Flow separation Boundary layer Liquid rocket engines Side forces	Unclassified-unlimited Curtis L. Bailey

19. SECURITY CLASSIF. (of this report)	20. SECURITY CLASSIF. (of this page)	21. NO. OF PAGES	22. PRICE
Unclassified	Unclassified	32	NTIS

ACKNOWLEDGMENTS

This research was performed under the NRC Resident Research Associateship Program of the National Academy of Sciences at the Astronautics Laboratory, Propulsion and Thermodynamics Division, NASA Marshall Space Flight Center (MSFC), Huntsville, Alabama. The encouragement given by C. R. Bailey, Scientific Advisor, K. W. Gross, H. G. Paul, Division Chief, and D. Pryor during the tenure is highly appreciated.

TABLE OF CONTENTS

LIST OF ILLUSTRATIONS

LIST OF SYMBOLS

Symbols	Definition
c_p	specific heat at constant pressure
C	constant
C_D	drag coefficient
C_F	thrust coefficient
d	diameter
D_1	drag per unit length
F	thrust
i	trip number
I	momentum
M	Mach number
p	pressure
R	gas constant
S	stagnation pressure ratio
T	temperature
u	velocity
x	distant from throat
y	coordinate normal to wall
γ	isentropic exponent
δ	boundary layer thickness

LIST OF SYMBOLS (Concluded)

Symbol	Definition
ΔF	thrust loss
Δp	pressure change
ϵ	expansion ratio
ν	viscosity
ρ	density
Θ	wall angle

Subscripts

a	ambient
c	combustion chamber
e	boundary layer edge
i	minimum pressure point (startpoint of the separation region ≈ trip location)
n	nozzle
ot	without trip
r	recovery
st	stagnation
t	throat
tw	trip
w	wall
wt	with trip

TECHNICAL MEMORANDUM X-64843

A PROCEDURE FOR CALCULATION OF BOUNDARY LAYER TRIP PROTUBERANCES IN OVEREXPANDED ROCKET NOZZLES

SUMMARY

Side forces occur during rocket engine start and shutdown in ambient pressures greater than zero. These forces are caused by non-axisymmetrical flow separation. One method of avoiding this undesirable effect is by using a boundary layer trip to force a clean, axisymmetrical separation line.

Since boundary layer disturbances generate shock waves and reduce nozzle performance, boundary layer trip sizing must represent a compromise between performance reduction and trip effectiveness. Procedures for calculating trip sizes, required positions, scaling effects and performance reduction plus a comparison between theory and available experimental data are presented.

INTRODUCTION

During rocket engine start and shutdown in ambient pressures greater than zero, nonaxial thrust components act as side loads on rocket nozzle walls. These unsteady, randomly oriented side forces are caused by unsymmetrical flow separation, and can impose a requirement for additional structural support thereby increasing the weight of the engine and mountings. Since such weight increases are undesirable, several methods of reducing the magnitude of the side forces have been proposed. [1]

One method of reducing side loads is to force clean, axisymmetric separation lines. This can potentially be accomplished through the use of boundary layer trips such as secondary injection, wall angle discontinuities, circumferential grooves, and circumferential trip protuberances. The use of a protuberance can be accomplished by installing a trip wire which has an advantage that it can usually be installed after the development of an engine and nozzle without any change of the basic configuration.

Any protuberance of a nozzle wall generates drag losses and shock waves which reduce engine performance. Since the size of the protuberance or trip wire affects the flow separation behavior, performance reduction and flow separation characteristics are related. A trip wire sizing and positioning procedure is required, therefore, to provide the combination of precise separation and minimum performance reduction.

This report describes one method for sizing, scaling, and positioning of trip protuberances. Some experimental results are presented, allowing a comparison between theory and experiment. The main purpose however, is to outline the rationale of the proposed calculation method.

TRIP WIRE SIZING

The objective in using trip wires is to achieve a forced separation of the flow. This separation should always occur at a higher wall pressure than without a trip wire. One or more trip wires in a nozzle are used as shown in Figure 1. During transient start and shutdown, the chamber pressure is lower than during main stage operation and the flow separates from the wall. At a given chamber pressure, the gases expand into the nozzle and flow over the trip wires, 1 to i - 1. At trip wire i, the flow disturbance is sufficient that the flow separates. Without a wire installed, the flow would have separated further downstream in the nozzle. When the chamber pressure is increased, the gases finally overflow this trip wire. Then the next wire, i+1, has been positioned such that at i+1 forced separation is achieved. A further increase of the chamber pressure lets the flow jump to wire i+2 and at last the nozzle flows full.

Although this approach of having many or an almost "continuous" series of trip wires along the nozzle wall seems to be promising, some of the disadvantages accrued appear to favor the use of only one or a few trip wires. The performance loss increases with the number of trip wires, and the change of the flow field over the trip is so severe that a certain distance between the trip wires is required so that the disturbances can decay.

The flow separation process is a boundary layer effect. Therefore, a short description of the boundary layer model, which is used for calculations, is necessary.

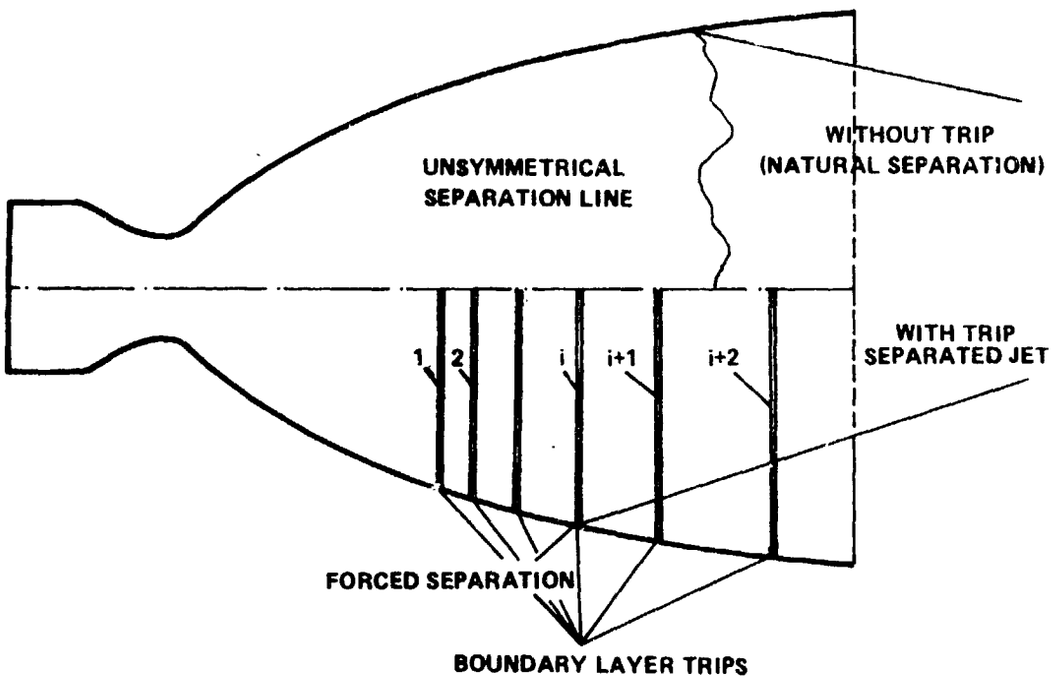

Figure 1. Nozzle flow separation, with and without boundary layer trips.

Boundary Layer Model

The boundary layer which approaches the trip wire is presented in Figure 2, together with the associated nomenclature. Since performance efficiency requires a small trip size, a trip height of about 1/10 of the boundary layer thickness should not be greatly exceeded. Therefore the distribution of flow properties at the boundary layer edge is of little interest.

The usual assumption for the velocity profile within the boundary layer is a 1/7 power law. Denoting the velocity as u, the velocity at the boundary layer edge as u_e, the boundary layer thickness as δ, and the coordinate normal to the wall as y, this distribution is expressed by:

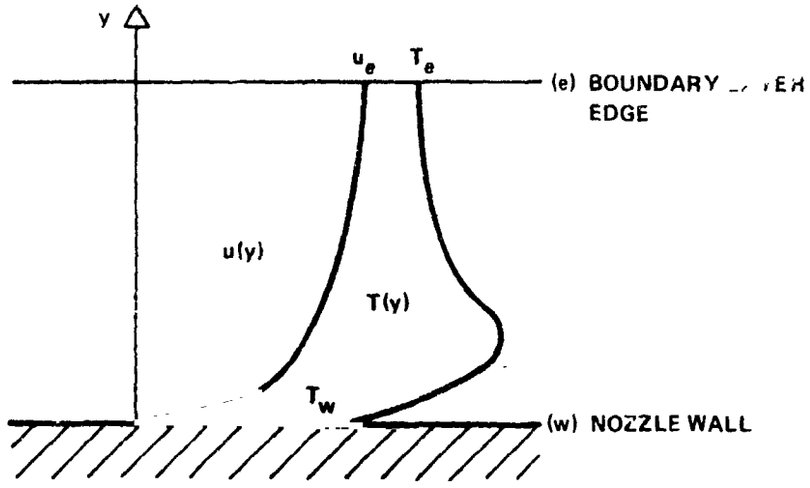

Figure 2. Boundary layer model.

$$\frac{u}{u_e} = \left(\frac{y}{\delta}\right)^{1/7} \quad . \tag{1}$$

The existence of a laminar sublayer will be neglected within the accuracy of this calculation.

The temperature distribution can be related to the velocity distribution by the Crocco equation:

$$\frac{T_{st} - T_w}{T_r - T_w} = \frac{u}{u_e} \quad ; \tag{2}$$

where, T_{st} is the local stagnation temperature, T_r is the stagnation temperature at the boundary layer edge, and T_w is the wall temperature. Since T_r is only slightly different from the combustion chamber temperature T_c, with the energy equation

$$T = T_{st} - \frac{u^2}{2\,c_p} \quad , \tag{3}$$

the local static temperature T can be obtained from:

$$T = \frac{u}{u_e}\left(T_c - T_w\right) + T_w - \frac{u^2}{2c_p} \quad . \tag{4}$$

Rearranging with the static temperature at the boundary layer edge

$$T_e = \frac{T_c}{1 + \frac{\gamma-1}{2} M_e^2} \quad , \tag{5}$$

yields

$$T = T_c \left[\frac{T_w}{T_c} + \frac{u}{u_e}\left(1 - \frac{T_w}{T_c}\right) - \left(\frac{u}{u_e}\right)^2 \frac{\frac{\gamma-1}{2} M_e^2}{1 + \frac{\gamma-1}{2} M_e^2} \right] \quad . \tag{6}$$

In these equations, M_e describes the Mach number at the boundary layer edge and γ the isentropic exponent of the gases, which are assumed to be ideal.

Upstream of the trip outside of its influential range a constant static pressure across the boundary layer is assumed. With the gas equation the density ρ is expressed by

$$\rho = \frac{p}{R\,T} \quad , \tag{7}$$

where p represents the static pressure and R the gas constant.

Performance Loss

The estimation of the performance loss by the trip protuberances requires some assumptions. The trip wire is small compared with the boundary layer and therefore the shock, which is generated in front of the disturbance, becomes weaker towards the boundary layer edge and should disappear. Then the wall pressure further downstream of the trip deviates only slightly from the undisturbed wall pressure and the performance loss due to wall pressure reduction can be neglected. With this assumption, the performance loss is generated only by the drag of the trip wire.

The drag is normally calculated by the dynamic pressure and a suitably defined drag coefficient C_D. Since the velocity and density upstream of the trip varies normal to the wall, an integration is necessary. Then the drag per length D_1 is (Fig. 3)

$$D_1 = \int_0^{d_{tw}} C_D(y) \frac{\rho}{2} u^2 \, dy \quad . \tag{8}$$

In C_D all effects such as low pressure at the back side of the trip protuberance are included. With the equations (6) and (7), the drag can be expressed by

$$D_1 = \int_0^{d_{tw}/\delta} C_D \frac{\delta \, p \, u_e^2 \left(\frac{u}{u_e}\right)^2 d\left(\frac{y}{\delta}\right)}{2R \, T_c \left[\frac{T_w}{T_c} + \frac{u}{u_e}\left(1 - \frac{T_w}{T_c}\right) - \left(\frac{u}{u_e}\right)^2 \frac{\frac{\gamma-1}{2} M_e^2}{1 + \frac{\gamma-1}{2} M_e^2}\right]} \tag{9}$$

In order to simplify the calculations, a constant, properly defined C_D is useful. An approximate value can be obtained from the various drag measurements of different body shapes. Rearranging with the boundary layer edge velocity of sound and equations (1) and (7) results in

$$D_1 = C_D M_e^2 p \frac{\gamma}{2} \frac{\delta}{1 + \frac{-1}{2} M_e^2} \int_0^{d_{tw}/\delta} \frac{\left(\frac{y}{\delta}\right)^{2/7} d\left(\frac{y}{\delta}\right)}{\frac{T_w}{T_c} + \left(\frac{y}{\delta}\right)^{1/7} \left(1 - \frac{T_w}{T_c}\right) - \left(\frac{y}{\delta}\right)^{2/7} \frac{\frac{\gamma-1}{2} M_e^2}{1 + \frac{\gamma-1}{2} M_e^2}} \tag{10}$$

The exact integration of equation (10) requires the use of a decomposition to partial fractions. An approximate solution can be obtained by the fact that above a distance of 0.01 δ, the integrand of (10) increases rather linearly.

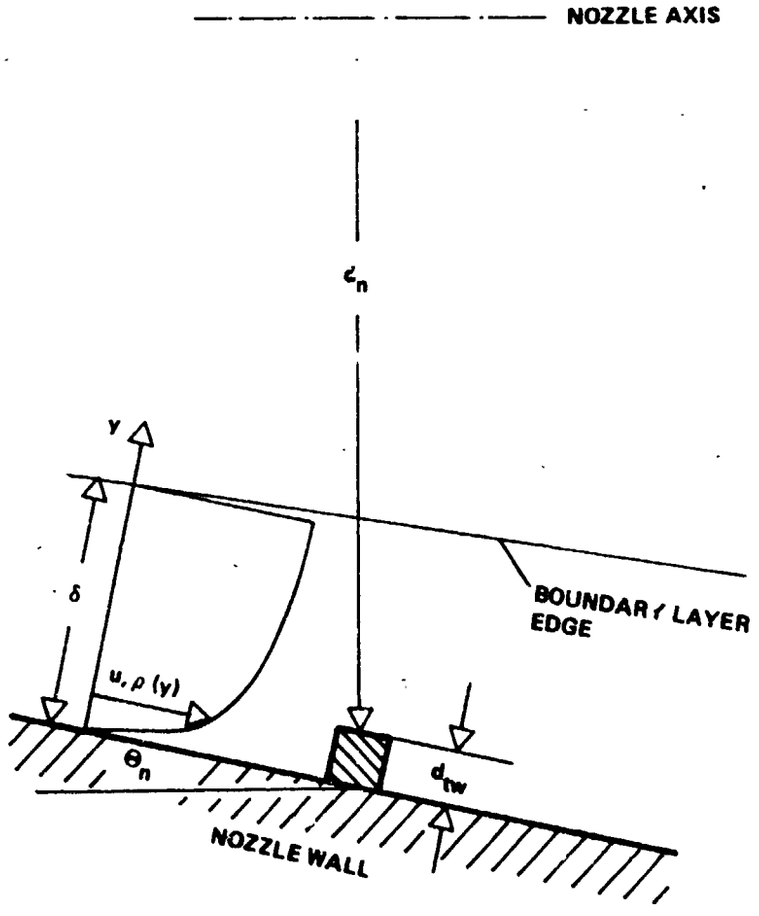

Figure 3. Trip protuberance and boundary layer.

Therefore, equation (10) can be written with little error

$$D_1 = C_D M_e^2 \left(\frac{0.5 p \gamma d_{tw}}{1 + \frac{\gamma-1}{2} M_e^2} \right) \left[\frac{\left(\frac{d_{tw}}{k\delta} \right)^{2/7}}{\frac{T_w}{T_c} + \left(\frac{d_{tw}}{k\delta} \right)^{1/7} \left(1 - \frac{T_w}{T_c} \right) - \left(\frac{d_{tw}}{k\delta} \right)^{2/7} \frac{\frac{\gamma-1}{2} M_e^2}{1 + \frac{\gamma-1}{2} M_e^2}} \right] . \quad (11)$$

The factor k represents the rather linear increase of ρu with y/δ in the region discussed and has a value of 0.5.

For a quick estimation of the second term on the right side of equation (11), some typical numbers for the different symbols are:

$$M_e = 3$$
$$d_{tw}/\delta = 0.1$$
$$T_w/T_c = 0.5$$
$$\gamma = 1.25$$

and equation (11) yields

$$D_1 = C_D M_e^2 \frac{0.35 \, p \gamma \, d_{tw}}{1 + \frac{\gamma-1}{2} M_e^2} . \quad (12)$$

The thrust loss is obtained by multiplying the drag per unit length with the nozzle perimeter, using only the axial component. With the nozzle diameter d_n and the wall angle Θ_n, the thrust loss ΔF_{tw} can be expressed by

$$\Delta F_{tw} = D_1 \pi d_n \cos \Theta_n . \quad (13)$$

The previous listed typical values can be used for a simple, approximate equation of the thrust loss. Assuming a drag coefficient of 0.8, which is similar to those for spheres or cylinders, equations (12) and (13) result in

$$\Delta F_{tw} = 0.5\, M_e^2\, p\, d_{tw}\, d_n \quad . \tag{14}$$

Equation (14) indicates that only very small trip sizes lead to negligible performance loss.

Wire Size and Flow Separation

A turbulent boundary layer in a rocket nozzle can only withstand a certain overexpanded condition. This condition is expressed by the separation criterion, which describes the ratio of the minimum full flowing wall pressure p_i to the ambient pressure p_a. The use of a trip changes this behavior, always achieving separation at a higher wall pressure than would be achieved without a trip.

Although the natural separation phenomenon in an overexpanded rocket nozzle is far from being solved completely, certain methods are available which describe the experimentally observed results reasonably well.[1] The theory, which was derived by Crocco and Probstein [2], achieves the best agreement with test data. The numerical results of this theory and the available separation data of hot firing nozzles are plotted in Figure 4.

The calculation of the relation between trip protuberance size and separation behavior can be done by a momentum approach.[2] The control volume, which is used for the analysis, agrees with that of Crocco-Probstein

1. Schmucker, R. H.: Status of Flow Separation Prediction in Liquid Propellant Rocket Nozzles. NASA TM X (to be published), Marshall Space Flight Center, Alabama 35812.

2. Another method for the determination of size effect on separation behavior is presented in the Appendix. This approach is based on the suggestion that the shock waves in the boundary layer change within a small region of the wall pressure, so that separation can occur.

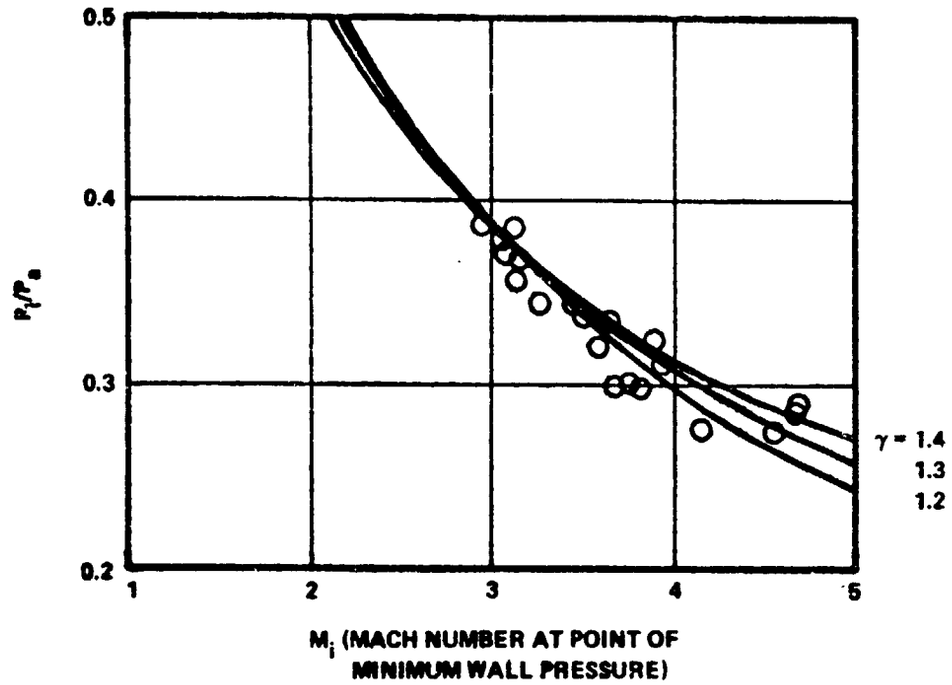

Figure 4. Experimental flow separation data and Crocco-Probstein flow separation criterion (Data points represent averaged hot firing data).

[2], and is presented in Figure 5. The momentum balance between the point i, which is upstream of the trip, and a point downstream of the trip (which is described by the subscript a for convenience), yields:

$$I_i - I_a - D_1 = \delta_i \left(p_a - p_{i_{wt}} \right) \quad , \tag{15}$$

where I is the momentum and the subscript wt describes the condition "with trip". Without a trip, equation (15) is written

$$I_i - I_a = \delta_i \left(p_a - p_{i_{ot}} \right) \quad , \tag{16}$$

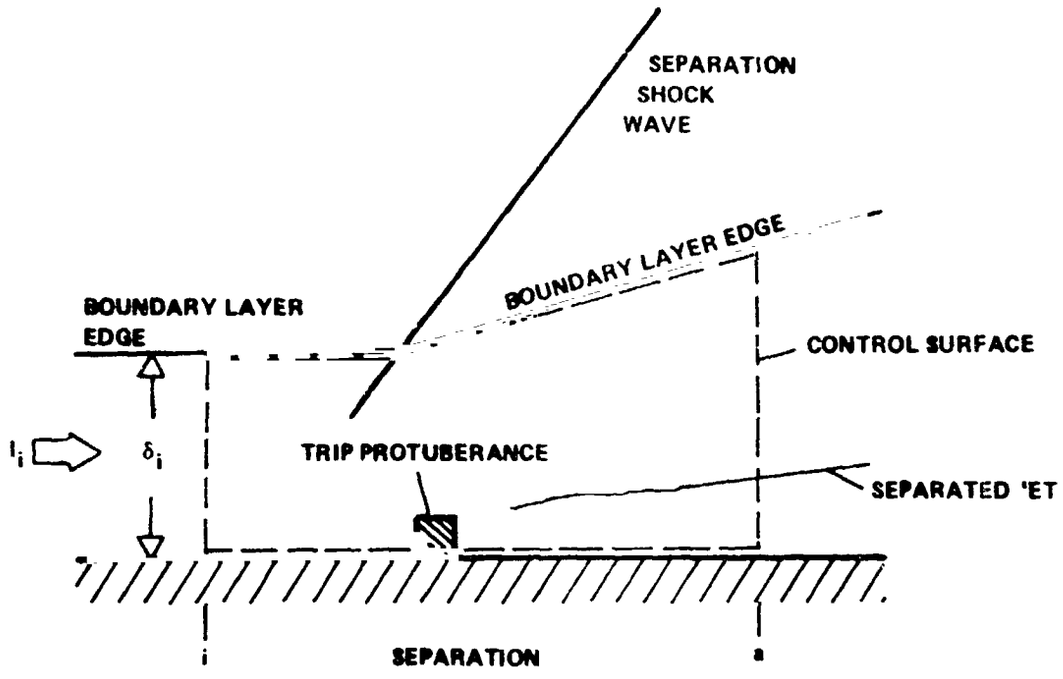

Figure 5. Control volume for trip size calculation.

with subscript ot as "without trip". The latter condition corresponds to normal separation in a nozzle. Combining equations (15) and (16) results in

$$\frac{p_{i_{wt}}}{p_a} = \frac{p_{i_{ot}}}{p_a} + \frac{D_1}{\delta_i p_a} \quad . \tag{17}$$

The pressure in equation (11) for the protuberance drag is the undisturbed pressure upstream of the trip. Relating the wire drag in equation (17) to this pressure results in

$$\frac{p_{i_{wt}}}{p_a} = \left(\frac{p_{i_{ot}}}{p_a}\right)\left(\frac{1}{1 - \frac{D_1}{\delta_i p_{i_{wt}}}}\right) \quad . \tag{18}$$

The separation conditions with a trip protuberance are calculated by using equation (18), the boundary layer data, and the separation data without trip. The latter can be obtained from Figure 4.

Equation (18) indicates a rather linear relation between the separation pressure change $p_{i_{wt}} - p_{i_{ot}}$ and the wire size, normalized with the boundary layer thickness. With increased wall cooling, the effectiveness of the trip increases since the density of combustion gases near to the wall is increased.

The combination of equation (18) and (12), together with numerical values allows the derivation of a simple, approximate equation for a rough estimation of the trip effect

$$\frac{p_{i_{wt}}}{p_a} = \left(\frac{p_{i_{ot}}}{p_a}\right)\left(\frac{1}{1 - 0.16\, M_i^2 \frac{d_{tw}}{\delta_i}}\right) \quad , \tag{19}$$

M_i is the Mach number at the boundary layer edge at the trip location (at point i).

The inversion of equation (18) allows the calculation of the trip size for a desired separation pressure change. Since the trip drag of equation (11) depends on the 1/7 and 2/7 power of a trip size, only an iterative solution is possible. A simple approximation is obtained by equation (19), using Δp_{tw} for the pressure increase,

$$\frac{d_{tw}}{\delta_i} = \left(\frac{1}{1 + \frac{p_{i_{ot}}}{\Delta p_{tw}}}\right)\left(\frac{6.25}{M_i^2}\right) \quad . \tag{20}$$

Equation (20) shows a strong influence of the Mach number, indicating a decrease of the normalized wire size along the nozzle wall. But since the boundary layer thickness increases with the length, the absolute value of the trip size increases also.

In Figure 6, some experimental data together with theoretical calculation are presented. The test data are obtained from a 4k H_2/LOX engine at NASA's Marshall Space Flight Center. They represent the minimum wall pressure $p_{i_{wt}}$ during the test. Since this nozzle was uncooled and therefore changed its temperature during the tests, the calculations were performed for two wall temperature ratios.

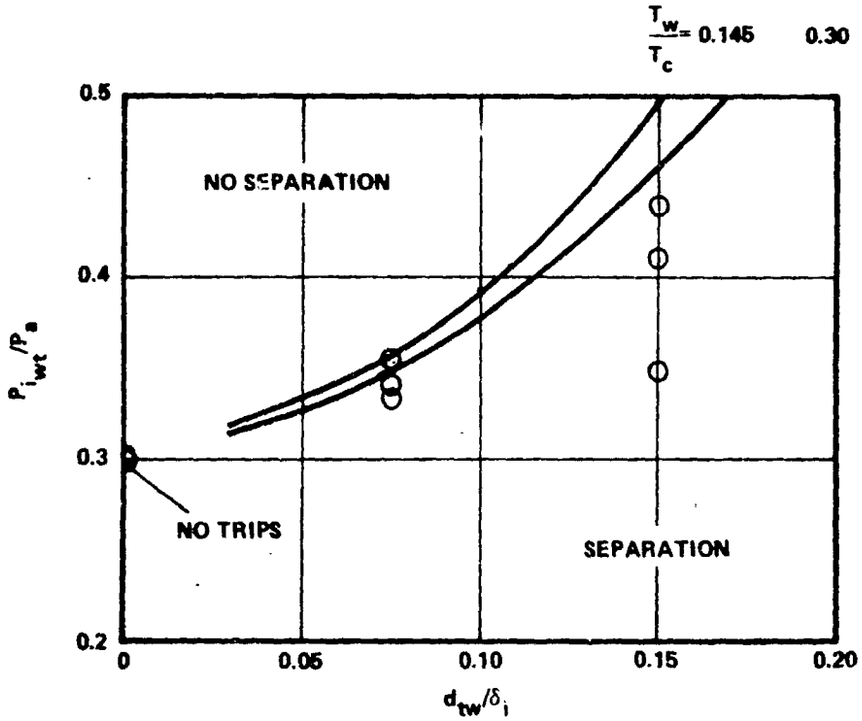

Figure 6. Calculated and measured separation pressure ratio (M_i=3.6, γ=1.26) (Test data obtained with NASA-MSFC 4-k H_2/O_2 engine).

The agreement between theory and experiment is rather good. The theoretical calculated values represent an upper limit, which is not exceeded by the test data. The measured separation pressures are normally lower than the theoretical limit, since the trip location does not agree with the upper trip position. (See later discussion of Trip Protuberance Position.) The test data

with the smaller trip size agree with the theoretical line. This indicates that the test results should be very sensitive to boundary layer changes. During these tests the separation point jumped from one trip to the next, and was probably caused by the wall temperature increase.

SCALING OF TRIP PROTUBERANCE

The performance loss and effectiveness depends on the drag of the trip protuberance. The exact numbers and relations of drag coefficient, velocity, and temperature distribution are not known. The measurement of separation behavior avoids this difficulty, since integral quantities in equations (14) and (20) are obtained.

For a measured separation pressure ratio and a fixed Mach number and trip shape, equation (20) can be simplified and the trip size is

$$d_{tw} = C_1 \delta_i \quad . \tag{21}$$

The trip protuberance height is a certain fraction of the boundary layer thickness. If the boundary layer thickness is known, the required size is obtained from equation (21) using test results for C_1.

If no boundary layer data are available, a rough estimation is possible using the boundary layer thickness of a flat plate. For convenience a conical nozzle is assumed (Fig. 7). Then, with the length x which starts at the throat, the boundary layer thickness can be written [3]

$$\delta_i = 0.37 \left(\frac{\nu}{u_i}\right)^{0.2} x^{0.8} \quad ; \tag{22}$$

where u_i is the velocity at the boundary layer edge, δ_i is the boundary layer thickness at the trip location i, and ν is the viscosity. The length x can be approximated by

$$x = \frac{d_n}{2 \sin \Theta_n} \quad . \tag{23}$$

Introducing the thrust equation

$$F = p_c \, d_t^2 \, \frac{\pi}{4} \, C_F \quad , \tag{24}$$

where d_t describes the throat diameter and C_F the thrust coefficient, thus yielding:

$$x = \left(\frac{F}{p_c}\right)^{0.5} \frac{\epsilon^{0.5}}{C_F^{0.5} \sin \Theta_n \, \pi^{0.5}} \quad . \tag{25}$$

Combining (22) and (25) results in

$$d_{tw} = \left(\frac{F}{p_c}\right)^{0.4} C_2 \quad , \tag{26}$$

where all constants are comprised in C_2. The trip wire size increases with the 0.4th power of thrust and decreases in the same way with chamber pressure.

The previous described scaling procedure is only valid for scaling to a different engine with the same boundary layer conditions. A scaling to other conditions, such as expansion ratio ϵ, Mach number, etc., requires a change of the constant C_2. These effects can be estimated by the proportionality

$$C_2 \sim \frac{\epsilon^{0.4} \left(1 + \frac{\gamma - 1}{2} M_i^2\right)}{C_F^{0.4} u_i^{0.2} M_i^2} \quad , \tag{27}$$

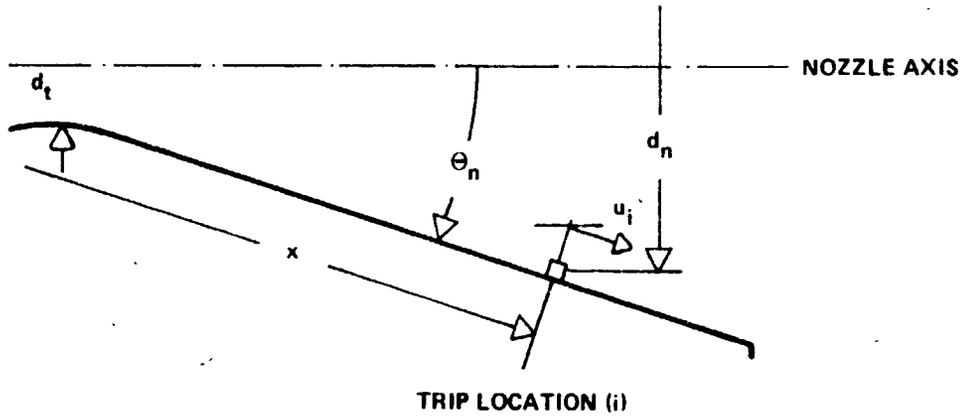

Figure 7. Geometry of a conical nozzle.

but the accuracy of such an approach is very questionable. Equation (27) should therefore only be used for the estimation of trends.

TRIP PROTUBERANCE POSITION

The calculation of the trip protuberance size requires, besides the wall temperature and the Mach number, the desired wall pressure at which the flow separates. It is obvious that this condition can only be fulfilled at a certain chamber pressure. During transient conditions, the chamber pressure changes and the trip device is only effective during a certain chamber pressure range. Therefore, the trips have to be positioned such that natural separation cannot occur anywhere.

For calculation of the possible location range for the trip protuberance, Figure 8 can be used. At a certain chamber pressure, an undisturbed wall pressure profile is obtained like that of Figure 8. According to the wall pressure distribution, a Mach number can be calculated at every station and, with the data of Figure 4, the natural separation pressure can be plotted. The intersection of the wall pressure profile and the separation pressure profile describes the natural separation point. Since a deviation from these ideal values always occurs, a small scatter must be introduced to get reliable numbers. Assuming a certain trip size allows, together with the local boundary layer thickness and wall temperature, the calculation of the trip drag. With the separation pressure and equation (18), this leads to the separation pressure

with trip. The intersection of this distribution with the undisturbed wall pressure results in the upper limit for the trip position. Placing the trip upstream of this point would result in a reattachment of the flow after the trip. The use of a trip protuberance downstream of the lower limit does not effect the natural flow separation at all. Therefore, a trip wire of a fixed size should only be placed in this described range.

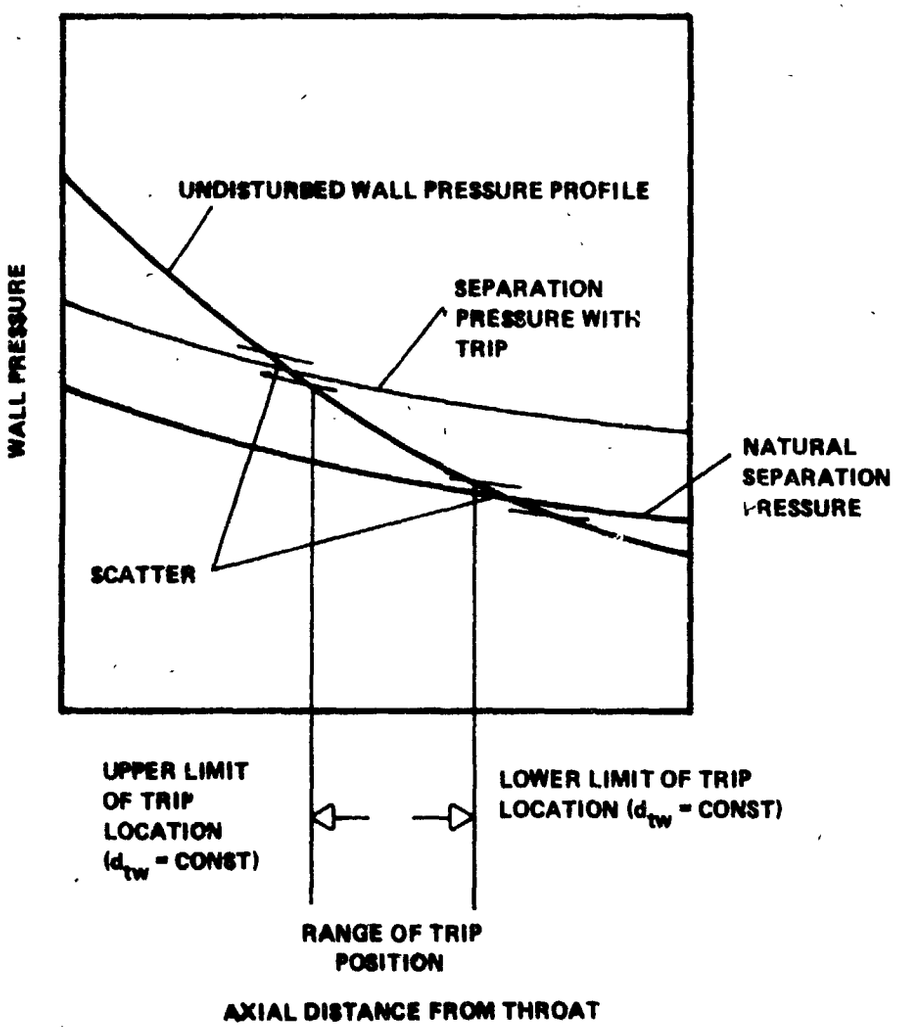

Figure 8. Position of trip protuberance (d_{tw} = const).

A changing chamber pressure varies only the undisturbed wall pressure profile. If the trip is positioned in the previous mentioned region of the nozzle, an increasing chamber pressure moves the condition to the upper limit. Finally the chamber pressure is high enough that the gases overflow the trip. In this case, at the lower limit of the trip location, a new trip device has to be located so that natural separation can be avoided. This holds true for every trip protuberance. The nozzle exit can also be considered as a trip.

The separation pressure increase with trip depends on the trip size. Smaller trips are less effective and require a larger number of devices. Bigger trips allow larger spacing and are not so sensitive to boundary layer changes. This favors the suggestion that for flow separation with trips, only a few or even one trip wire should be used.

CONCLUSION

Boundary layer trip protuberances are a promising approach for side load reduction in overexpanded rocket nozzles by forcing a clean, axisymmetrical separation line. Effectiveness can easily be verified by installing a circumferential trip wire.

A sizing, scaling, and positioning procedure for the trip protuberances is described, and is based on the momentum equation. This derivation indicates that performance loss and trip effectiveness are related. The performance loss is very sensitive to trip size, but only very small trips are necessary for the significant change of the separation behavior. Some experimental data are presented, which show good agreement with the theoretical results. This suggests that the theory presented describes the real phenomena rather well.

The scaling of trips requires some information about the boundary layer. A simplified scaling procedure relates thrust, chamber pressure, and trip size for a fixed boundary layer condition. Positioning and spacing of trips is based on the natural separation behavior and the change caused by the trips. Larger spacing, which is desired for less boundary layer disturbance, can be achieved by a few bigger trips. The last trip has to be in such a position that the nozzle exit is being considered as a final trip.

APPENDIX

CALCULATION OF THE TRIP SIZE BY WALL PRESSURE CHANGE DUE TO SHOCKS

The flow field around the trip protuberance and the wall pressure distribution is presented in Figure A1. Upstream of the wire the flow is compressed and separates from the wall. A curve shock emerges in this region, decreasing in strength with increasing distance from the wall. The separated stream line reattaches at a certain point from the protuberance. In the separated region the wall pressure increases. Downstream of the first reattachment point the flow expands and the wall pressure drops. The trip size is so small that the area ratio of the nozzle can be considered as unchanged. Due to the shock wave the local stagnation pressure in the boundary layer drops. At a certain point from the trip protuberance, the flow separates again and the wall pressure drops. If the chamber pressure is high enough, the gases flow over this protuberance and reattach downstream of the trip. Therefore, a reattachment shock is generated, which leads to a further stagnation pressure loss. Since the disturbance of the flow field occurs only in a small region near to the wall, the mixing process damps the differences of the stagnation pressures and the deviation from the theoretical wall pressure profile decays very fast. The final pressure distribution should be slightly below the disturbed pressure profile, but the deviations are almost too small to be measured. (Wall pressure measurements in a small nozzle with rectangular trip wires do not show any deviation from the wall pressure without trips.) If the chamber pressure is low enough, the expansion downstream of the trip prevents a reattachment and a forced separation is achieved.

Downstream of each reattachment point the static wall pressure is lower than upstream of the wire since shock waves decrease the local stagnation pressure. This favors the suggestion that with a fixed trip configuration, a certain chamber pressure range exists which will always lead to forced separation. The lower limit of this range corresponds to separation at the edge of the trip.[3] The higher limit corresponds to the condition just before reattachment after the trip.

3. The flow always separates at the trip or upstream of the trip if the chamber pressure is lower than this lower limit. Therefore this chamber pressure must be considered as a theoretical lower limit.

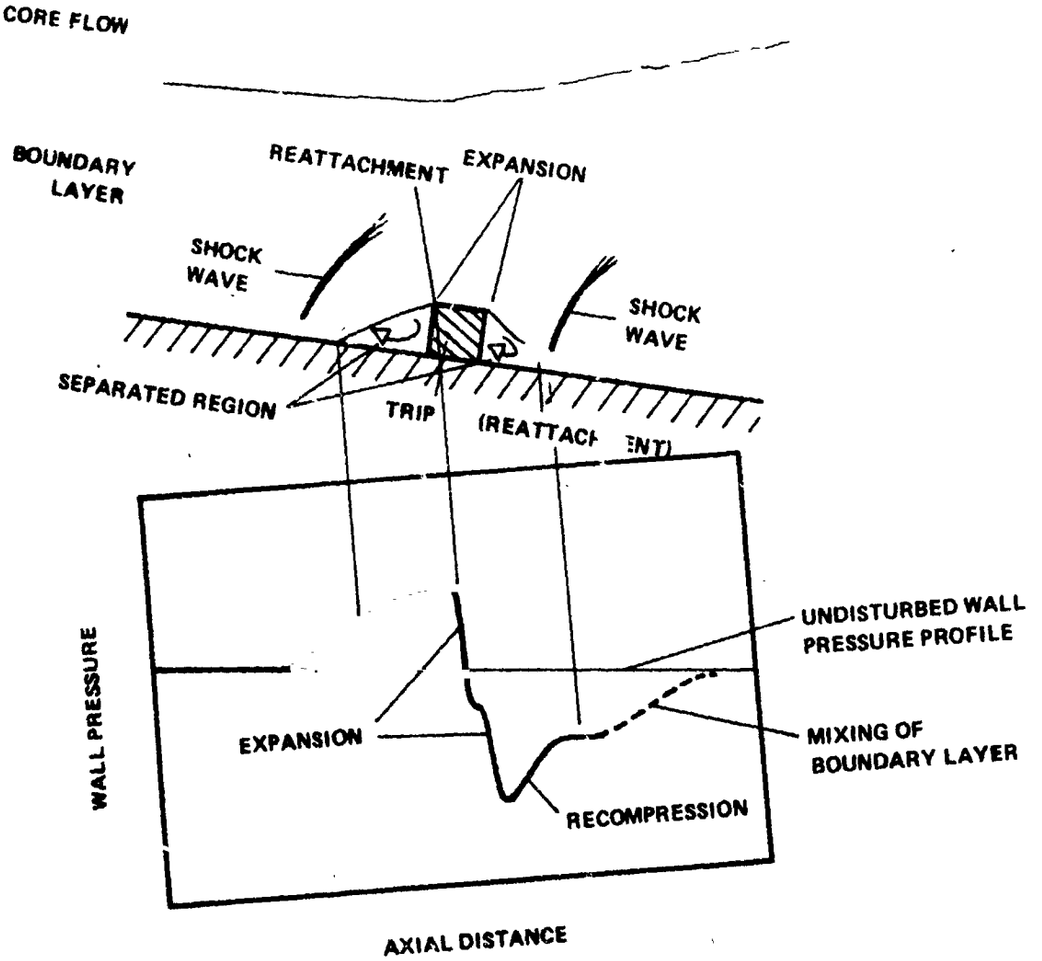

Figure A1. Flow field and pressure distribution at boundary layer trip.

For calculation of the trip size by the wall pressure change due to the shocks some assumptions have to be made. In Figure A2, the simplified flow field is presented. The details of pressure distribution near to the trip device can be neglected. The presence of a trip protuberance decreases the static wall pressure at or shortly downstream of the trip. The pressure drop Δp_{tw} is the result of a stagnation pressure decrease of that streamline, which is the same distance from the wall as the upper effective limit of the trip. The

pressure change is described by a normal shock. This can be considered as a mean between the previous mentioned upper and lower limit of the separation condition.

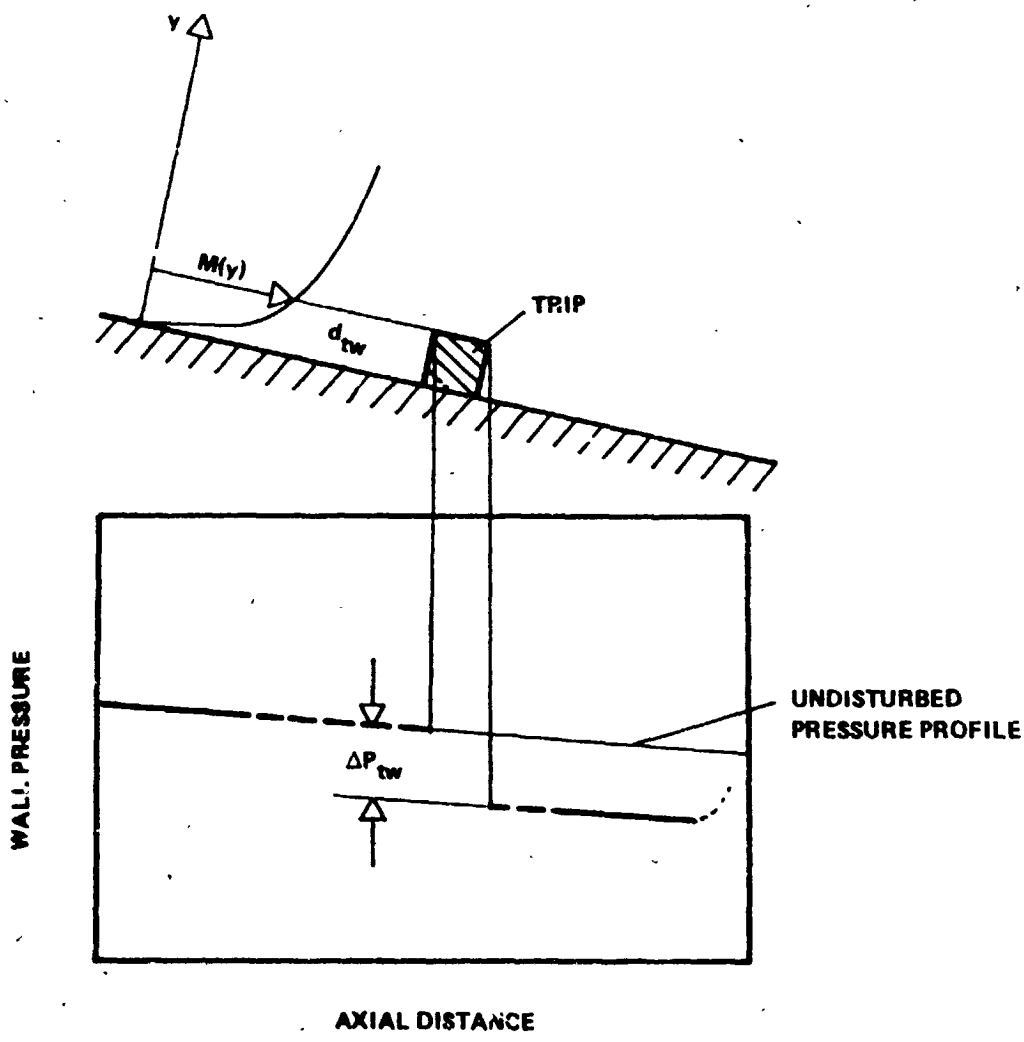

Figure A2. Simplified pressure distribution at trip.

Denoting S_{tw} as the stagnation pressure ratio of the trip edge stream line across the shock waves, the expression for the wall pressure is

$$\frac{p_{i_{wt}}}{p_a} = \left(\frac{p_{i_{ot}}}{p_a}\right)\left(\frac{1}{S_{tw}}\right) \quad . \tag{A1}$$

The stagnation pressure ratio is obtained by the usual shock relations [4],

$$S_{tw} = \left(\frac{\frac{\gamma-1}{2}M^2}{1+\frac{\gamma-1}{2}M^2}\right)^{\frac{\gamma}{\gamma-1}} \frac{1}{\left(\frac{2}{\gamma+1}M^2 - \frac{\gamma-1}{\gamma+1}\right)^{\frac{\gamma}{\gamma-1}}} \quad . \tag{A2}$$

In the interesting Mach number range this expression can be simplified by a linear relation,

$$S_{tw} = 1.45 \cdot M_i\, 0.36 \quad . \tag{A3}$$

The Mach number is calculated by equation (1), (6), and (7):

$$M = M_e \frac{\frac{u}{u_e}}{\left\{\left(1+\frac{\gamma-1}{2}M_e^2\right)\left[\frac{T_w}{T_c} + \frac{u}{u_e}\left(1-\frac{T_w}{T_c}\right) - \left(\frac{u^2}{u_e}\right)\frac{\frac{\gamma-1}{2}M_e^2}{1+\frac{\gamma-1}{2}M_e^2}\right]\right\}^{0.5}} \quad , \tag{A4}$$

and the pressure ratio with trip results in,

(A5)

M_i represents the boundary layer edge Mach number at the trip position.

A comparison of the results of equation (A5) with the test data of Figure 6 indicates that the assumption of a normal shock leads to discrepancies with the measurements. Although equation (A5) predicts rather small trip sizes and the correct trend of the wall temperature effect, the deviation from the real phenomenon is excessive. Therefore trip wire sizing based on shock generation is not an acceptable approach.

$$\frac{p_{i_{wt}}}{p_a} = \left(\frac{p_{i_{ot}}}{p_a}\right) \frac{1}{(1.45 - 0.36 M_i)\left\{\left(1 + \frac{\gamma-1}{2} M_i^2\right)\left[\frac{T_w}{T_c} + \left(\frac{d_{tw}}{\delta_i}\right)^{1/7}\left(1 - \frac{T_w}{T_c}\right) - \left(\frac{d_{tw}}{\delta_i}\right)^{2/7} \frac{\frac{\gamma-1}{2} M_i^2}{1 + \frac{\gamma-1}{2} M_i^2}\right]\right\}^{0.5}}$$

REFERENCES

1. Schmucker, R. H.: Side Loads in Liquid Rocket Engines. Paper presented at the first annual Research and Technology Review, NASA-MSFC, 1973.

2. Crocco, L.; and Probstein, R. F.: The Peak Pressure Rise Across an Oblique Shock Emerging From a Turbulent Boundary Layer Over a Plane Surface. Princeton University Report 254, March, 1954.

3. Eckert, E. G. R.; and Drake, R.: Mass and Heat Transfer. MacGraw Hill, New York, 1959.

4. Shapiro, A.: The Dynamics and Thermodynamics of Compressible Fluid Flow. The Ronald Press Company, New York, 1954.

APPROVAL

A PROCEDURE FOR CALCULATION OF BOUNDARY LAYER TRIP PROTUBERANCES IN OVEREXPANDED ROCKET NOZZLES

By Robert H. Schmucker

The information in this report has been reviewed for security classification. Review of any information concerning Department of Defense or Atomic Energy Commission programs has been made by the MSFC Security Classification Officer. This report, in its entirety, has been determined to be unclassified.

This document has also been reviewed and approved for technical accuracy.

A. A. McCool
Acting Director, Astronautics Laboratory

C. C. WOOD
Acting Chief, Propulsion and
Thermodynamics Division

J. A. LOMBARDO
Chief, Liquid Propulsion
and Power Branch

C. R. BAILEY
Chief, Propulsion
Thermosciences Section

☆ U.S. GOVERNMENT PRINTING OFFICE 1974 – 748 298 / 170 REGION NO. 4